THE ASTROPHYSICAL JOURNAL, 384:292–297, 1992 January 1

NH_3 AND NH_2 IN THE COMA OF COMET BRORSEN-METCALF

STEPHEN C. TEGLER AND LUKE F. BURKE
Department of Astronomy, University of Florida, Gainesville, FL 32611

SUSAN WYCKOFF AND MARIA WOMACK
Department of Physics and Astronomy, Arizona State University, Tempe, AZ 85287

AND

UWE FINK AND MICHAEL DISANTI[1]
Lunar and Planetary Laboratory, University of Arizona, Tucson, AZ 85721
Received 1991 January 11; accepted 1991 July 10

ABSTRACT

Narrow-band CCD images of comet Brorsen-Metcalf have been obtained using interference filters (fwhm = 20 Å) centered at $\lambda = 6250$ and 6338 Å to isolate continuum and NH_2 (8–0) $\tilde{A}\,^2A_1$–$\tilde{X}\,^2B_1$ emission, respectively. The 6338 Å images corrected for background sky and dust-scattered solar continuum isolate the NH_2 coma in the comet. The distribution of NH_2 is symmetric and shows no evidence for jet structure at the 3 σ significance level above background emission. An azimuthal average of the NH_2 image produces an NH_2 surface brightness profile for comet Brorsen-Metcalf which gives a factor of ~ 10 improvement in the signal-to-noise ratio over previous one-dimensional long-slit NH_2 observations, and provides a significant constraint on the NH_2 photodissociation time scale in comets.

A Monte Carlo simulation of the comet coma assuming that NH_3 is the primary source of NH_2 is described and compared with the observations. The effects on the surface brightness distribution of NH_2 due to (1) collisions in the inner coma and (2) non–steady state production rates were investigated with the Monte Carlo model. For an observed production rate, $Q(H_2O) \sim 7 \times 10^{28}$ molecules s^{-1}, collisional effects on the NH_3 and NH_2 outflow had at most a $\sim 10\%$ effect on the NH_2 surface brightness profile. The models also indicate that large variations in the gas production rate on time scales $\sim \tau_{NH_2}$ could cause significant differences from the steady state profiles. Because comet Brorsen-Metcalf showed no significant dust or gas production rate variability, we argue that steady state conditions best match the comet at the time of observations. We find for steady state conditions and a recently revised NH_2 photodissociation time scale, $\tau_{NH_2} \sim 3.3 \times 10^4$ s at 1 AU, a satisfactory match between the observed and computed NH_2 surface brightness profiles. For a steady state model with $\tau_{NH_2} \sim 5.0 \times 10^4$ s at 1 AU the observations are fitted to an estimated accuracy of $\sim 10\%$. We conclude that NH_3 is probably the dominant source of NH_2 in the coma of comet Brorsen-Metcalf. The conclusive identification of the NH_2 percursor in comets will require (1) the direct detection of NH_3, (2) observations of NH_2 emission over several successive nights to monitor possible production rate variations, or (3) accurate experimental photodissociation cross sections for NH_2.

Subject headings: comets: individual (Brorsen-Metcalf) — molecular processes

1. INTRODUCTION

A primary goal in the study of cometary ices is to identify and describe the environment in which the ices condensed. The possible condensation environments range from a dense interstellar cloud to the proto–solar nebula. The ammonia (NH_3) ice abundance in comets is a key to identifying and describing this environment (Lunine 1989). However, NH_3 has not yet been detected spectroscopically in a comet. Furthermore, the *Giotto* spacecraft flyby of comet Halley yielded controversial results on the NH_3 abundance. Specifically, Allen et al. (1987) combined *Giotto* mass spectrometer data and a chemical model of comet Halley's coma to obtain $NH_3/H_2O = 1\%$–2%, while Marconi & Mendis (1988) found the *Giotto* mass spectrometer data to be consistent with no NH_3 in the coma. Since the photodissociation of NH_3 into NH_2 has a 95% branching ratio (Allen et al. 1987), an alternative method to test for the existence of NH_3 in comets is to compare an observed NH_2 surface brightness distribution with a calculated NH_2 surface brightness distribution that assumes NH_3 is the dominant source of NH_2. Here we present evidence consistent with NH_3 ice in the nucleus of comet Brorsen-Metcalf as the source of the observed NH_2. Specifically, we show that an image of comet Brorsen-Metcalf's NH_2 coma agrees with a calculated image that assumes the observed NH_2 coma is produced by the photodissociation of NH_3.

2. OBSERVATIONS

Comet Brorsen-Metcalf is a periodic comet ($P \sim 70$ yr) in a prograde orbit. This comet has one of the lowest known dust/gas ratios (e.g., Brooke, Tokunaga, & Knacke 1990). We observed comet Brorsen-Metcalf on 1989 August 7 UT using the Catalina site of the University of Arizona Observatories, the Lunar and Planetary Laboratory CCD camera, and two narrow-band (fwhm = 20 Å) interference filters having central wavelengths $\lambda_c = 6338$ and 6250 Å. The observation time was

[1] Postal address: NASA/Goddard Space Flight Center, Planetary Systems Branch, Greenbelt, MD 20771.

shared with a spectroscopic project comparing the composition of comet Brorsen-Metcalf with that of comet Halley (DiSanti & Fink 1991). At the time of observation comet Brorsen-Metcalf's heliocentric and geocentric distances were 0.93 and 0.62 AU, respectively. The comet images were bias subtracted, flat-fielded, extinction corrected, and registered. Star trails were also removed from the images. The 6338 Å images isolated the NH_2 (8–0) band and included contributions from sky brightness and the comet's continuum. The 6250 Å images isolated the comet's continuum and included a contribution from sky brightness. The images taken through the 6338 Å filter were summed, resulting in a single image with an 1800 s exposure time. Similarly, the images taken through the 6250 Å filter were summed, also resulting in a single image with an 1800 s exposure time. Contamination of the images by [O I] emission lines at 6300 and 6363 Å is negligible since the filters transmit less than 1% of the incident light at these wavelengths.

In order to obtain a pure NH_2 image we have subtracted the comet and sky continua from the 6338 Å image of comet Brorsen-Metcalf. We describe the image subraction here. Data numbers detected in pixels of the 6338 Å image, $C_{\mathrm{bm},6338}$, can be approximated by

$$C_{\mathrm{bm},6338} = (F_{\mathrm{nh2},6338} + F_{\mathrm{con},6338} + F_{\mathrm{sky},6338}) \times T_{6338}\,\Delta\lambda_{6338}\,S_{6338}\,At\ , \quad (1)$$

where $F_{\mathrm{nh2},6338}$ is the NH_2 flux at 6338 Å from comet Brorsen-Metcalf, $F_{\mathrm{con},6338}$ is the continuum flux at 6338 Å, $F_{\mathrm{sky},6338}$ is the sky at 6338 Å, T_{6338} is the peak transmission of the 6338 Å filter, $\Delta\lambda_{6338}$ is the fwhm of the 6338 Å filter, S_{6338} is the overall system efficiency at 6338 Å dominated by the quantum efficiency of the CCD, A is the area of the telescope aperture, and t is the exposure time. Similarly, data numbers detected in pixels of the 6250 Å image, $C_{\mathrm{bm},6250}$, can be approximated by

$$C_{\mathrm{bm},6250} = (F_{\mathrm{con},6250} + F_{\mathrm{sky},6250})T_{6250}\,\Delta\lambda_{6250}\,S_{6250}\,At\ , \quad (2)$$

where $F_{\mathrm{con},6250}$ is the continuum flux at 6250 Å, $F_{\mathrm{sky},6250}$ is the sky flux at 6250 Å, T_{6250} is the peak transmission of the 6250 Å filter, $\Delta\lambda_{6250}$ is the fwhm of the 6250 Å filter, and S_{6250} is the instrument efficiency at 6250 Å. From direct spectra of comet Brorsen-Metcalf (DiSanti & Fink 1991) as well as solar fluxes (Neckel & Labs 1984) and a sky spectrum (Broadfoot & Kendall 1968), we have determined that spectral gradients in the comet and sky continua between 6338 and 6250 Å are negligible, that is, $F_{\mathrm{con},6338} \simeq F_{\mathrm{con},6250}$ and $F_{\mathrm{sky},6338} \simeq F_{\mathrm{sky},6250}$. From equations (1) and (2) and negligible spectral gradients in the comet and sky continua, a pure NH_2 image is obtained by subtracting the 6250 Å image from the 6338 Å image after correcting for differences in transmission of the filters and response of the CCD. We have corrected for these differences by observing the solar analog star BS 9107. We have bias subtracted, sky subtracted, flat-fielded, and extinction corrected the 6338 and 6250 Å images of BS 9107. Following equations (1) and (2) the values for data numbers detected from BS 9107 at 6338 and 6250 Å are approximated by

$$C_{\mathrm{bs},6338} = F_{\mathrm{bs},6338}\,T_{6338}\,\Delta\lambda_{6338}\,S_{6338}\,At \quad (3)$$

and

$$C_{\mathrm{bs},6250} = F_{\mathrm{bs},6250}\,T_{6250}\,\Delta\lambda_{6250}\,S_{6250}\,At\ . \quad (4)$$

Since $F_{\mathrm{bs},6338} \simeq F_{\mathrm{bs},6250}$, the ratio of the data numbers detected at 6338 Å to the data numbers detected at 6250 Å is given by

$$\frac{C_{\mathrm{bs},6338}}{C_{\mathrm{bs},6250}} = \frac{T_{6338}\,\Delta\lambda_{6338}\,S_{6338}}{T_{6250}\,\Delta\lambda_{6250}\,S_{6250}}\ . \quad (5)$$

From the BS 9107 images we have measured

$$\frac{T_{6338}\,\Delta\lambda_{6338}\,S_{6338}}{T_{6250}\,\Delta\lambda_{6250}\,S_{6250}} = 0.92\ . \quad (6)$$

We have multiplied the 6250 Å image of comet Brorsen-Metcalf by 0.92 and subtracted this scaled 6250 Å image from the 6338 Å image to obtain a pure NH_2 image. We point out that using a solar analog star also removes the assumption that $F_{\mathrm{con},6338} \simeq F_{\mathrm{con},6250}$ as long as the continuum reflectivity of the comet is flat. This is the case for comet Brorsen-Metcalf (DiSanti & Fink 1991).

In Figure 1 we show a contour map of the 6338 Å image prior to background sky and comet continuum subtraction. The contours represent 200, 250, 500, 750, and 1000 data numbers per pixel, respectively. Pixels near the edge of the image have values of ~180 data numbers per pixel and represent the per pixel brightness of the sky. The image scale is 0.″93 pixel^{-1}, corresponding to 420 km pixel^{-1} at the comet. The image has dimension 1.68×10^5 km on a side. In Figure 2 we show the scaled 6250 Å image. Contour levels in the 6250 Å image represent 200, 250, and 500 data numbers per pixel. The sky brightness per pixel, the scale size, and the image dimensions are the same as in Figure 1. In Figure 3 we present a contour map of the pure NH_2 (8–0) image. The contour levels in Figure 3 represent 25, 50, 100, 250, 500, 750, and 1000 data numbers per pixel. The scale size and image dimensions are the same as in Figures 1 and 2.

In the morphology of these images, we see that the NH_2 image prior to continua subtraction (Fig. 1) and the continuum image (Fig. 2) are brighter in the antisolar direction (the Sun is located at the top of the images). This asymmetry is due to scattering of solar photons by grains in the dust tail. In con-

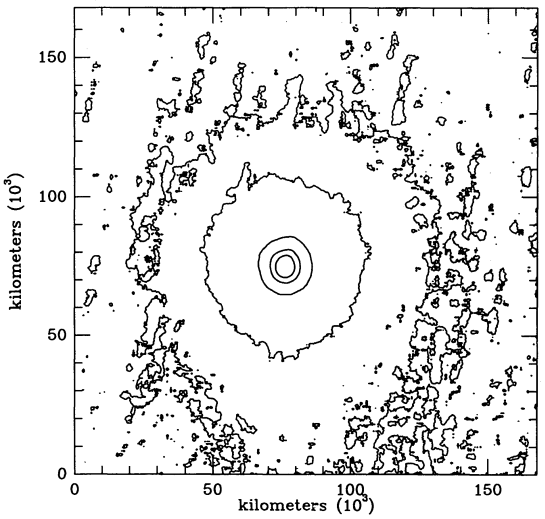

FIG. 1.—Image of comet Brorsen-Metcalf taken through the λ_c = 6338 Å filter prior to continuum and sky brightness subtraction. Contour levels represent 200, 250, 500, 750, and 1000 data numbers per pixel (sky brightness ~180 data numbers per pixel). Direction to the Sun is up.

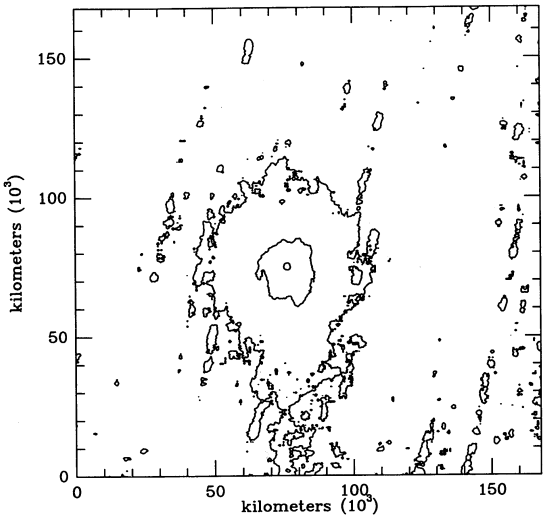

FIG. 2.—Image of comet Brorsen-Metcalf's continuum coma. Contour levels represent 200, 250, and 500 data numbers per pixel (sky brightness ~180 data numbers per pixel). Residual star trails are seen at the lowest contour level. Direction to the Sun is up.

trast to Figures 1 and 2 the difference image, representing a pure NH_2 gas coma (Fig. 3), is symmetric.

3. THE MODEL

We have calculated images of comet Brorsen-Metcalf's NH_2 coma using a Monte Carlo method. The Monte Carlo method uses normalized probability densities to simulate systems that are difficult or impossible to describe with closed analytical or simple numerical solutions. The basis of the Monte Carlo method is given by

$$\int_0^x f(x')dx' = R_i\,, \tag{7}$$

where R_i is a computer-generated random number between 0 and 1, x represents a physical parameter, and $f(x)$ is the probability that x has a value between x and $x + dx$. For a known probability density, $f(x)$, and a generated random number, equation (7) gives a value for the physical parameter x. Details of the application of the Monte Carlo method to particle transport are given by Carter & Cashwell (1975). The Monte Carlo method has been applied previously to cometary atmospheres by Combi & Delsmme (1980), Kitamura, Ashihara, & Yamamota (1985), Combi & Smyth (1988), and Tegler (1989). In the model presented here we assume that

$$NH_3 + h\nu \rightarrow NH_2 + H \tag{8}$$

and

$$NH_2 + h\nu \rightarrow NH + H \tag{9}$$

are responsible for the creation and destruction of NH_2 molecules.

To obtain the simulated NH_2 coma images we calculate the individual trajectories of 10^6 NH_3 parent molecules and the resulting NH_2 daughter molecules in the following manner. Consider a time interval of length T_F where we specify the start of the interval to be $t = 0$ and the end of the interval to be $t = T_F$. At time t_i, where $0 \leq t_i \leq T_F$, the ith NH_3 molecule is released from the nucleus. We assume a time-independent production rate, that is, that the NH_3 molecule has equal probability of being released at any instant within the time interval. Thus, $f(x)$ in equation (7) is a constant, $1/T_F$, and the time of release of the NH_3 molecule is given by a random number, $R_{i,t}$, and

$$t_i = R_{i,t}\, T_F\,. \tag{10}$$

The three-dimensional trajectory of the released NH_3 molecule is specified by spherical polar angles, ϕ_i and θ_i, with origin at the nucleus of the comet. We assume the NH_3 molecule has equal probability of being released in any direction into the solid angle $d\Omega$. Thus, $f(x)$ in equation (7) is $d\Omega/4\pi$. In spherical coordinates

$$\frac{d\Omega}{4\pi} = \frac{\sin\theta\, d\theta}{2}\,\frac{d\phi}{2\pi}\,. \tag{11}$$

We see in equation (11) that $f(\theta, \phi) = f(\theta)\, f(\phi)$ and hence θ and ϕ are independent random variables. Thus we write

$$\phi_i = 2\pi R_{i,\phi} \tag{12}$$

and

$$\cos\theta_i = 1 - 2R_{i,\theta}\,. \tag{13}$$

The generation of these two random numbers, $R_{i,\phi}$ and $R_{i,\theta}$, along with an assumed speed of 1 km s^{-1} (Schloerb et al. 1986) completely specifies the NH_3 molecule's initial trajectory.

The model tracks the trajectory of the NH_3 molecule until it is photodissociated at time $t_i + t_{NH_3}$ where t_{NH_3} is given by

$$t_{NH_3} = -\tau_{NH_3}\, r^2 \ln(R_{NH_3,i})\,. \tag{14}$$

In equation (14) $R_{NH_2,i}$ is a random number, r is the comet's heliocentric distance in AU, and τ_{NH_3} is the photodissociation time scale of an NH_3 molecule in the solar radiation field, at 1

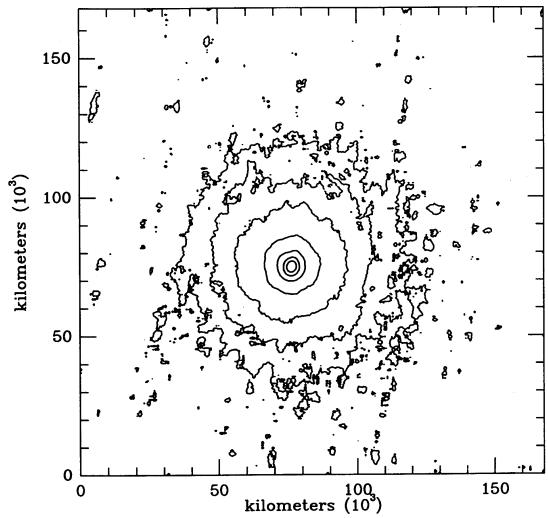

FIG. 3.—Image of comet Brorsen-Metcalf's NH_2 (8–0) coma after sky and continuum subtraction. Contour levels represent 25 (3 σ), 50, 100, 250, 500, 750, and 1000 data numbers per pixel. Residual star trails are seen at the lowest contour level. Direction to the Sun is up.

AU. This time scale is given by

$$\tau_{NH_3} = \left(\int_0^{\lambda} \sigma_{NH_3,\lambda} F_{\lambda} d\lambda \right)^{-1}, \quad (15)$$

where $\sigma_{NH_3,\lambda}$ is the photodissociation cross section for NH_3 and F_{λ} is the solar ultraviolet flux. Photodissociation cross sections for NH_3 are well studied and are taken from Samson, Haddad, & Kilcoyne (1987), Suto & Lee (1983), Thompson, Harteck, & Reeves (1963), and Watanabe (1954). The solar ultraviolet flux is taken from measurements made by the *Solar Mesosphere Explorer* satellite. (*SME*; G. Rottman 1989, private communication). We obtain $\tau_{NH_3} = 7.7 \times 10^3$ s at 1 AU which agrees with Allen et al. (1987) and Schmidt et al. (1988). In this calculation neither changes in the UV flux distribution with solar activity nor a possible Swings effect due to the comet's changing heliocentric velocity, as suggested by the data of Fink, Combi, & Disanti (1991), have been included.

After the NH_3 molecule photodissociates, the velocity of the NH_2 molecule is determined by conservation of energy and momentum requirements. In the reference frame of the NH_3 molecule, that is, the center of momentum reference frame, we have

$$\frac{hc}{\lambda} - D - I = \frac{m_H v_H^2}{2} + \frac{m_{NH_2} v_{NH_2}^2}{2} \quad (16)$$

and

$$m_H v_H = m_{NH_2} v_{NH_2}, \quad (17)$$

where λ is the wavelength of the photon that photodissociates the NH_3 molecule, D is dissociation energy of the NH_3 molecule, I is the energy imparted to the internal degrees of freedom of the NH_2 molecule, v_{NH_2} and v_H are the speeds of the NH_2 molecule and the H atom in the center of momentum reference frame, and m_{NH_2} and m_H are the masses of the NH_2 molecule and the H atom. Biesner et al. (1988) have measured the internal energy, I, of an NH_2 molecule following laser excitation of NH_3 into its $\tilde{A}\,^1A_2'' \; v_2' = 0$ and 1 states. They show that the NH_2 molecule is produced in the lowest electronic and vibrational states, but in highly excited rotational states. Biesner et al. find $0 \leq I \leq 1$ eV. For $D = 4.645$ eV (Biesner et al.) and $\lambda = 2000$ Å, we obtain $v_{NH_2} = 1.0$ and 0.6 km s^{-1} for $I = 0$ and 1 eV, respectively. The velocity of the NH_2 molecule in the reference frame of the comet nucleus is given by the vector sum of the velocity of the NH_2 molecule in the center of momentum reference frame and the velocity of the NH_3 molecule (center of momentum velocity). We take v_{NH_2} to be 0.8 km s^{-1} from the above arguments. Conservation of momentum and energy do not constrain the direction of v_{NH_2}, and hence the NH_2 molecule has equal probability of being released in any direction into the solid angle $d\Omega$. Therefore, two random numbers and equations (12) and (13) determine the direction of v_{NH_2}. As stated above we take the velocity of the NH_3 molecule to be 1 km s^{-1} and directed radially away from the nucleus.

The NH_2 molecule leaves the photodissociation site and follows a linear trajectory at constant speed until it photodissociates at time $t_i + t_{NH_3} + t_{NH_2}$ where t_{NH_2} is given by

$$t_{NH_2} = -\tau_{NH_2} r^2 \ln (R_{NH_2,i}) \quad (18)$$

and $R_{NH_2,i}$ is a random number, r is the comet's heliocentric distance in AU, and τ_{NH_2} is the photodissociation time scale of the NH_2 molecule, at 1 AU.

To the author's knowledge no experimental photodissociation cross sections have been measured for NH_2. Thus, theoretical cross sections (Saxon, Lengsfield, & Liu 1983) have been used to calculate two values for the NH_2 photodissociation time scale in comets. Using equation (15) (with $\sigma_{NH_2,\lambda}$ substituted for $\sigma_{NH_3,\lambda}$), we obtain $\tau_{NH_2} = 5.3 \times 10^5$ s and $\tau_{NH_2} = 3.3 \times 10^4$ s at 1 AU. The two photodissociation time scales are calculated from the theoretical cross sections of Saxon, Lengsfield, and Liu, where the longer time scale was calculated using the photodissociation cross sections for the two lowest lying channels of NH_2 at 1620 and 1780 Å. Two additional photodissociation channels at 1100 and 1300 Å were added by E. van Dishoeck (1990, private communication), which significantly decreased the NH_2 photodissociation time scale to 3.3×10^4 s (1 AU). The 1100 and 1300 Å channels contribute equally and together control the photodissociation of NH_2 in comets. The shorter photodissociation time scale has been used in analyzing recent cometary data (e.g., Wyckoff, Tegler, & Engel 1991). We will calculate NH_2 images using both NH_2 time scales.

The position of the NH_2 molecule in the reference frame of the nucleus is calculated for time T_F. The calculation described here is repeated for the remaining 10^6 NH_3 molecules. Only parent NH_3 molecules and daughter NH_2 molecules with $t_i + t_{NH_3} \leq T_F$ and $t_i + t_{NH_3} + t_{NH_2} \geq T_F$ have NH_2 positions calculated. These temporal constraints demand that the NH_3 molecule has been photodissociated, and the NH_2 molecule has not been photodissociated at the time the calculation ceases, T_F. The set of NH_2 molecule positions at time T_F is the model calculated NH_2 image.

We have not considered elastic molecule–molecule collisions. We show here that elastic collisions have little effect on our NH_2 surface brightness distributions. The collision zone radius, r_c, is defined to be the distance from the nucleus at which the path length between collisions is equal to the distance from the nucleus,

$$r_c = \frac{Q\sigma}{4\pi v}, \quad (19)$$

where Q is the H_2O production rate, σ is the collision cross section, and v is the gas outflow velocity. Roettger et al. (1990) observed comet Brorsen-Metcalf on 1989 August 5 and measured $Q = 6.7 \times 10^{28}$ molecules s^{-1}. A similar water production rate of 7.0×10^{28} molecules s^{-1} was observed a few days earlier (August 2) by DiSanti & Fink (1991) during the same observing run as the present data. For σ we make the approximation that the collision cross section between molecules is given by the sum of the individual atomic cross sections determined from individual atomic radii. For H_2O–H_2O collisions we calculate $\sigma = 5 \times 10^{-25}$ km^2. We take $v = 1$ km s^{-1}. Substitution of these values into equation (19) gives $r_c \sim 3.0 \times 10^3$ km for comet Brorsen-Metcalf on August 7. The time scale for an NH_3 molecule to photodissociate (6.7×10^3 s) is more than 2 times longer than the time necessary for the NH_3 molecule to reach the collision zone radius (3×10^3 s). Therefore, an NH_2 molecule is more likely to be produced outside the collision zone. Since $0.6 \leq v_{NH_2} \leq 1.0$ km s^{-1} and the NH_3 radial outflow velocity is $\simeq 1$ km s^{-1}, an NH_2 molecule is not likely to have a trajectory directed inward toward the collision zone. Thus, an NH_2 molecule is unlikely to collide with another molecule after being produced. NH_3 molecules will collide with other molecules. However, the collision zone radius is approximately the same size as the spatial resolution

of our observations. We have calculated an NH_2 image that includes elastic molecule–molecule collisions and find that this image differs by $\leq 10\%$ from an image calculated with the collisionless model described here. The collisional Monte Carlo model for NH_3 and NH_2 molecules is described by Tegler (1989) and Tegler & Wyckoff (1991).

4. DISCUSSION

In this section we compare the observed and calculated NH_2 images. Since both the observed and calculated images appear symmetric, we compute and present surface brightness profiles to reduce the noise. The profiles were obtained by computing the average data numbers within concentric annuli of radial size 0.″93, about the central pixel. The filled circles in Figure 4 represent the observed NH_2 surface brightness profile. The error bars represent the systematic effect on the profile due to the uncertainty in the sky brightness. Specifically, the error bars represent the uncertainty in the contribution of night-sky air glow to the 6250 and 6338 Å narrow-band filters. We estimated the uncertainty in the air glow from a sky spectrum by Broadfoot & Kendall (1968) and from long-slit spectra (DiSanti & Fink 1991; Fink et al. 1991). The random error may be estimated from the scatter of the points. In Figure 4 the solid line and the dotted line represent calculated NH_2 profiles for collisionless Monte Carlo models with $\tau_{NH_2} = 3.3 \times 10^4$ and $\tau_{NH_2} = 5.3 \times 10^5$ s, respectively.

An NH_2 profile calculated assuming an NH_3 source (τ_{NH_3}) and $\tau_{NH_2} = 3.3 \times 10^4$ s agrees with the observed NH_2 profile within the uncertainties of the observed profile. An NH_3 source with $\tau_{NH_2} = 5.3 \times 10^5$ s is predicted to have a significantly more extended NH_2 surface brightness profile than observed. The models presented here have been calculated assuming that the molecular production rate is constant. Tegler (1989) pointed out that the NH_2 profile is significantly affected by changes of factors of 2–3 in the gas production rate. It is possible to obtain agreement between the observed and the calculated profiles of NH_2 with an NH_3 source, and assuming $\tau_{NH_2} = 5.3 \times 10^5$ s, if we also assume a time-dependent gas production rate. Unfortunately, we do not have data on August 6 or 8 to constrain the time variability of comet Brorsen-Metcalf's gas production rate. However, observations by others indicate that comet Brorsen-Metcalf was a very inactive comet, exhibiting little variability in both gas and dust production other than the monotonic dependence on heliocentric distance (Lynch et al. 1990; Roettger et al. 1990). Therefore, it is highly unlikely that the NH_2 production rate was changing by factors of 2–3 on time scales ≤ 1 day near the time of our observations.

We also present in Figure 4 an NH_2 profile calculated with a collisional Monte Carlo model that assumes an NH_3 source, $\tau_{NH_2} = 3.3 \times 10^4$ s, and elastic collisions between NH_3 and H_2O molecules (*long dash line*). Clearly, collisions have at most $\sim 10\%$ effect on the NH_2 surface brightness profile of comet Brorsen-Metcalf.

We have calculated NH_2 profiles using a collisionless Monte Carlo model with τ_{NH_2} as a free parameter. We find the best match between the observed and calculated NH_2 radial profiles occurs for a calculated profile with $\tau_{NH_2} = 5.0 \times 10^4$ s, the solid line in Figure 5. Thus, if the NH_2 coma in comet Brorsen-Metcalf results from a constant rate of sublimation of NH_3 ice and the error in the sky brightness subtraction is small, then Figure 5 indicates that the photodissociation time scale of NH_2 molecules at 1 AU may be closer to 5.0×10^4 s than to 3.3×10^4 s. This result is in good agreement with a recent analysis of scale lengths for comet Halley by Fink et al. (1991). Fitting Haser models to their data, these authors found preperihelion NH_2 parent and daughter scale lengths of 3.8×10^3 km and 7.9×10^4 km, respectively. Preperihelion values are used for comparison because the preperihelion heliocentric velocity of comet Halley (-25 km s^{-1}) is close to the preperihelion value of comet Brorsen-Metcalf (-29 km s^{-1}), and Fink et al. found a significant velocity dependent pre- and postperihelion asymmetry in the NH_3 and NH_2 scale lengths. With the outflow speed of 1 km s^{-1} used in the present paper the above scale lengths translate into lifetimes of $\sim 3.8 \times 10^3$ s

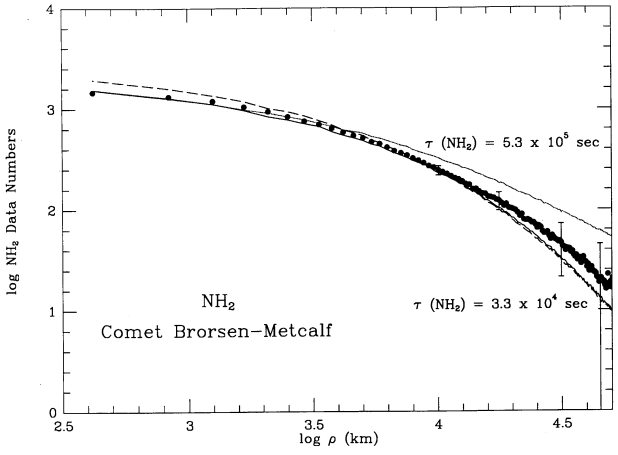

FIG. 4.—Observed NH_2 surface brightness profile (*filled circles*) compared with Monte Carlo simulations. Calculated NH_2 surface brightness profiles using collisionless model for an NH_3 source and dissociation product, NH_2, with lifetimes, $\tau_{NH_2} = 3.3 \times 10^4$ s (*solid line*), and $\tau_{NH_2} = 5.3 \times 10^5$ s (*dotted line*). Monte Carlo model including effects of collisions for NH_3 dissociating into NH_2 with a lifetime, $\tau_{NH_2} = 3.3 \times 10^4$ s (*long dash line*). Error bars represent a systematic error as explained in text. Figure demonstrates that the shorter NH_2 lifetimes fit the observations significantly better than the longer one.

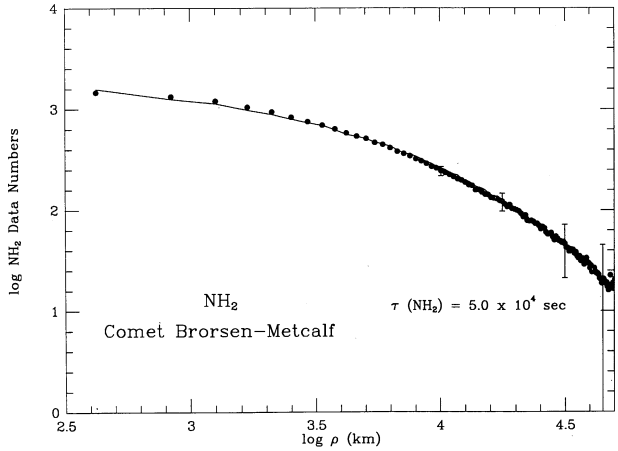

FIG. 5.—Observed NH_2 surface brightness profile (*filled circles*). Calculated NH_2 surface brightness profile using collisionless model and assuming an NH_3 source and $\tau_{NH_2} = 5.0 \times 10^4$ s (*solid line*).

for NH_3 and $\sim 8 \times 10^4$ s for NH_2; the latter is close to the best-fit value of 5×10^4 s in this paper.

Previous observations of the NH_2 surface brightness distribution in comets were obtained from long-slit spectra rather than narrow-band imaging data and had much lower signal-to-noise ratios (Delsemme & Combi 1983; Johnson, Fink, & Larson 1984; Wyckoff et al. 1988). We have been able to perform a detailed observation-model comparison because we have obtained such a high signal-to-noise level in our NH_2 data presented here and because we have incorporated recently determined molecular parameters which are necessary in the modeling of the NH_2 coma. Thus, our observational data have been used to significantly constrain the NH_2 photodissociation time scale.

Our NH_2 image in Figure 3 shows no evidence of jets or other asymmetries at the 3 σ level above background sky and continuum. Jets were observed in CN images of comet Halley (A'Hearn et al. 1986). The lack of NH_2 jets is consistent with NH_3 ice sublimating from the nucleus as the dominant source of the observed NH_2. Our observations cannot rule out a semi-volatile organic compound slowly released from grains as a very minor source, accounting for $\leq 3\%$ of the NH_2.

We conclude that an image of the NH_2 coma in a comet with a good signal-to-noise ratio can be modeled by assuming an NH_3 source and using either a constant NH_3 production rate and a short NH_2 photodissociation lifetime or a variable NH_3 production rate and a long NH_2 photodissociation lifetime. Further observational work should strive to obtain NH_2 images on consecutive nights to constrain the effects of time variability. In addition, an experimental determination of NH_2 photodissociation cross sections is urgently needed to better determine the NH_2 photodissociation time scale, a key parameter in the calculated NH_2 images.

We thank Michael A'Hearn for his useful comments on the manuscript. We also gratefully acknowledge the able assistance of W. Grundy at the telescope. This research is supported by NASA grants NAGW-2296 to H. C., NAGW-574 to S. W., NAGW-1549 to U. F., and the University of Florida Division of Sponsored Research.

REFERENCES

A'Hearn, M. F., Hoban, S., Birch, P. V., Bowens, C., Martin, R., & Klinglesmith, D. A. 1986, Nature, 324, 649
Allen, M., et al. 1987, A&A, 187, 502
Biesner, J., Schnieder, L., Schmeer, J., Ahlers, G., Xie, X., Welge, K. H., Ashford, M. N. R., & Dixon, R. N. 1988, J. Chem. Phys., 88, 3607
Broadfoot, A. L., & Kendall, K. R. 1968, J. Geophys. Res., 73, 426
Brooke, T. Y., Tokunaga, A. T., & Knacke, R. F. 1990, in Proc. Workshop on Observations of Recent Comets, ed. W. F. Huebner, J. Rahe, P. A. Wehinger, & I. Konno (San Antonio: Southwest Research Institute), 97
Carter, L. L., & Cashwell, E. D. 1975, Particle-Transport Simulation with the Monte Carlo Method (U. S. Energy Research and Development Administration) (Washington: GPO)
Combi, M. R., & Delsemme, A. H. 1980, ApJ, 327, 633
Combi, M. R., & Smyth, W. M. 1988, ApJ, 327, 1026
Delsemme, A. H., & Combi, M. R. 1983, ApJ, 271, 388
DiSanti, M. A., & Fink, U. 1991, Icarus, 91, 105
Fink, U., Combi, M. R., & DiSanti, M. A. 1991, ApJ, in press
Johnson, J. R., Fink, U., & Larson, S. M. 1984, Icarus, 60, 351
Kitamura, Y., Ashihara, O., & Yamamota, T. 1985, Icarus, 61, 278
Lunine, J. I. 1989, in The Formation and Evolution of Planetary Systems, ed. H. A. Weaver & L. Danly (Cambridge: Cambridge Univ. Press), 213
Lynch, D. K., Russel, R. W., Hanner, M. S., & Lien, D. J. 1990, in Proc. Workshop on Observations of Recent Comets, ed. W. F. Huebner, J. Rahe, P. A. Wehinger, & I. Konno (San Antonio: Southwest Research Institute), 70
Marconi, M. L., & Mendis, D. A. 1988, ApJ, 330, 513
Neckel, H., & Labs, D. 1984, Solar Phys., 90, 205
Roettger, E. E., Feldman, P. D., Budzien, S. A., A'Hearn, M. F., & Festou, M. C. 1990, in Proc. Workshop on Observations of Recent Comets, ed. W. F. Huebner, J. Rahe, P. A. Wehinger, & I. Konno (San Antonio: Southwest Research Institute), 59
Samson, J. A. R., Haddad, G. N., & Kilcoyne, L. D. 1987, J. Chem. Phys., 87, 6416
Saxon, R. P., Lengsfield, B. H., & Liu, B. 1983, J. Chem. Phys., 78, 312
Schloerb, F. P., Kinzel, W. M., Swade, D. A., & Irvine, W. M. 1986, ApJ, 310, L55
Schmidt, H. U., Wegmann, R., Huebner, & W. F., Boice, D. C. 1988, Comput. Phys. Comm., 49, 17
Suto, M., & Lee, L. C. 1983, J. Chem. Phys., 78, 4515
Tegler, S. C. 1989, Ph.D. thesis, Arizona State Univ.
Tegler, S. C., & Wyckoff, S. 1991, in preparation
Thompson, B. A., Harteck, P., & Reeves, R. R. 1963, J. Geophys. Res., 68, 6431
Watanabe, K. 1954, J. Chem. Phys., 22, 1564
Wyckoff, S., Tegler, S. C., & Engel, L. 1991, ApJ, 368, 279
Wyckoff, S., Tegler, S., Wehinger, P. A., Spinrad, H., & Belton, M. J. S. 1988, ApJ, 325, 927